J Neurophysiol 97: 2439–2447, 2007.
First published January 24, 2007; doi:10.1152/jn.00164.2006.

On Use of a Nominal Internal Model to Detect a Loss of Balance in a Maximal Forward Reach

Alaa A. Ahmed[1,3] and James A. Ashton-Miller[1,2,3]

Biomechanics Research Laboratory, [1]Departments of Biomedical and [2]Mechanical Engineering and [3]Institute of Gerontology, University of Michigan, Ann Arbor, Michigan

Submitted 15 February 2006; accepted in final form 17 January 2007

Ahmed AA, Ashton-Miller JA. On use of a nominal internal model to detect a loss of balance in a maximal forward reach. *J Neurophysiol* 97: 2439–2447, 2007. First published January 24, 2007; doi:10.1152/jn.00164.2006. We hypothesize that the CNS detects a loss of balance by comparing outputs predicted by a nominal, forward internal model with actual sensory outputs. When the resulting control error signal reaches an anomalously large value, this control error anomaly (CEA) signals a loss of balance and precedes any observable compensatory response. To test this hypothesis, a multi-input, multi-output internal model of a standing forward reach task was developed that incorporated on-line model identification and a Gaussian failure detection algorithm. Eleven healthy young women were then asked to stand and reach forward to a target positioned from 95 to 125% of their maximum reach distance. Kinematic and kinetic data were recorded at 100 Hz unilaterally from the upper body, leg, and foot. Evidence of successful CEA detection was a compensatory step between 100 ms and 2 s later. The results show that use of a threshold, set at 3 SD from the mean, on error in the control of leg segment acceleration detected a CEA and correctly predicted a compensatory response in 92.6% of 108 trials. Leg acceleration control error was a better predictor than upper body or foot acceleration control error ($P = 0.000$). CEA detection performed more reliably than loss of balance detection algorithms based on kinematic thresholds ($P = 0.000$). The results support the hypothesis that a loss of balance may be identified via the use of a nominal forward internal model and probabilistic error monitoring.

INTRODUCTION

Falls are a leading cause of both nonfatal injuries and injury-related death at any age, especially for adults over the age of 65 yr; (National Center for Injury Prevention and Control 2002; Rice and MacKenzie 1989). Every nonsyncopal unintentional fall is preceded by a "loss of balance." There is, however, a lack of consensus on what a loss of balance really is in conceptual, physical, or mechanistic terms.

In the field of postural control, a loss of balance has traditionally been held to occur when the whole-body center of gravity passes outside its base of support, or dynamically, when it cannot be brought to rest over the base of support (Pai and Patton 1997). Taking this view, the CNS appears to consider loss of balance to be a mechanical stability problem, dependent solely on the governing physical laws. This approach, however, cannot answer the question of how we, as humans, determine these stability limits, a priori, and plan our control movements. From a mechanical standpoint, determining these limits would require a model with knowledge of center of mass location, range of motion limits, and maximum torque capacities as well as base of support limits. Even then it would still be unable to account for our perception of environmental risk, sensory predictions, and even task familiarization, all of which have been shown to affect postural control and the initiation of compensatory responses (Cham and Redfern 2002; Eng et al. 1994; Pai et al. 2000). This paper addresses these issues by developing an alternative conceptual description of how the CNS might detect a loss of balance. Rather than focus on system outputs, as traditional approaches do, it emphasizes knowledge of the applied control input (efference copy) to the system.

We have proposed that a loss of balance is the fundamental requirement for the CNS to initiate a compensatory response aimed at preventing a potential fall and/or subsequent injury. Specifically, this on-demand correction is initiated when the control error between the predicted and actual outputs, resulting from a known control input, reaches an unusually large or anomalous value (Ahmed and Ashton-Miller 2004). The detection of this control error anomaly (CEA) involves the formation of a nominal, forward internal model, calculation of control error, and stochastic decision-making based on a Gaussian distribution. Initially, the control input is sent by the CNS to a nominal, forward internal model and the actual plant (Fig. 1). The nominal internal model characterizes the normal (predicted) output of the system in response to a given input in contrast to an internal model in the formal sense being an exact representation of the system. The nominal internal model is identified in real time and calculates the predicted output given the received control input. The control error is then calculated as the difference between the predicted and actual outputs, sensed via feedback to the sensory systems, and analyzed by a subcomponent of the controller called the "CEA detector." The CEA detector monitors the control error and compares it to the maximum allowable limits. A CEA is detected when the error signal exceeds a threshold set at 3 SD (3σ) beyond the mean of the baseline signal. Detection of CEA corresponds to the detection of a loss of balance and the subsequent need for a compensatory response. Thus once CEA is detected, any compensatory response that is initiated soon afterward is confirmatory evidence that the CNS had detected the loss of balance and therefore the need for this response. The first test of the CEA theory and the 3σ threshold was conducted and validated in a whole-body, 1 degree-of-freedom (df), chair-balancing

Address for reprint requests and other correspondence: J. A. Ashton-Miller, Biomechanics Research Laboratory, Department of Mechanical Engineering, University of Michigan, 3216 G. G. Brown, 2350 Hayward St., Ann Arbor, MI 48109-2125 (E-mail: jaam@umich.edu).

The costs of publication of this article were defrayed in part by the payment of page charges. The article must therefore be hereby marked "*advertisement*" in accordance with 18 U.S.C. Section 1734 solely to indicate this fact.

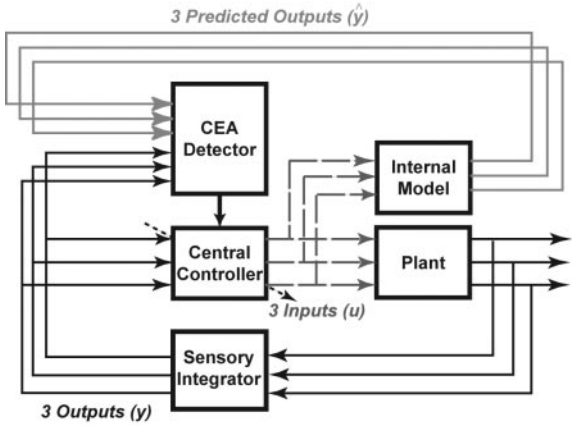

FIG. 1. Block diagram of multi-input, multi-output model and algorithm components: 3 predicted output signals (gray lines), 3 output signals (black), 3 input signals (dashed). The internal model calculates the predicted outputs based on the control inputs received from the central controller. Error between the predicted and actual outputs is calculated by the control error anomaly (CEA) detector. When the error reaches an anomalously large value, a CEA is detected and triggers an adaptive response in the central controller.

task performed by young adults (Ahmed and Ashton-Miller 2004). In a follow-up paper (Ahmed and Ashton-Miller 2005), it was observed that older adults responded prematurely to CEA while performing the same chair-balancing task.

The components of the proposed CEA theory, a nominal internal model, control error, and stochastic decision-making, build on ideas in biomechanics, postural control, cognitive, behavioral and computational neuroscience and the motor control fields. A critical assumption is that the detection of loss of balance, and the accompanying response, are mediated by higher centers in the CNS. There is evidence of cortical involvement in the execution and possibly the initiation of balance responses, as well as the maintenance of standing posture (Maki et al. 2001a,b; McIlroy et al. 1999; Ouchi et al. 1999). Moreover, forward internal models in the CNS have become familiar notions in the contemporary motor control literature with neuro-imaging and behavioral results suggesting they may reside in the cerebellum (Blakemore et al. 1998, 2001, 2003; Diedrichsen et al. 2005; Muller and Dichgans 1994). Such models have also been implicated in postural control (Loram et al. 2004; van der Kooij et al. 1999, 2001). There are also findings that support the idea in CEA theory that humans monitor how well they are controlling their movements (Hohwy and Frith 2004; Kerns et al. 2004). Finally, there is both behavioral and neurophysiological evidence to support the calculation, detection, and monitoring of conflict and error by the CNS (Botvinick et al. 2004; Kandel et al. 2000; Marr 1969). Based on these results, it seems reasonable to assume that the CNS calculates the error between predicted and actual sensory outcomes, monitors it, and may even alter control strategies based on it. With regard to stochastic decision making, there are at least two studies indicating that the CNS uses stochastic parameters to plan, control and adapt movements (Kording and Wolpert 2004; Lungu et al. 2004).

In the present paper, we extend CEA theory to include multiple body segments and then test its efficacy in detecting a loss of balance in a multi-degree of freedom forward reaching task. Reaching was selected because it is an activity of daily living involving the control of multiple body segments. The farther one has to reach, the more challenging the balancing task becomes and the greater the risk of a loss of balance. Perhaps partly for these reasons, the elderly consider reaching forward as one of the three most challenging activities of daily living (Powell and Myers 1995; Tinetti et al. 1990). Indeed, "functional reach" has been used as a potential test of postural stability for the elderly and as an indicator of fall risk (Duncan et al. 1990). Here, functional reach is defined as the maximal distance one can reach forward beyond arm's length in upright stance while maintaining a fixed base of support. In their initial study, Duncan et al. (1990) found that functional reach correlated positively with maximal center of pressure excursion, an established test of dynamic balance, and negatively with age.

By applying the CEA theory to the forward reach task, which involves the coordination of multiple body segments, we can examine its ability to generalize to a system with multiple inputs, multiple outputs, and multiple error signals (Fig. 1). In contrast to the single control error monitored in the single df chair task studied by Ahmed and Ashton-Miller (2004), the simplest sagittally symmetric model of the bimanual forward reach task would involve monitoring three control error signals, each corresponding to a degree of freedom (for example, rotation about the hip, ankle, and toe). The occurrence of a forward compensatory step is then an unambiguous and observable demonstration of an attempt to recover from a loss of balance.

In this paper, we test the primary hypothesis that a CEA can reliably predict an impending compensatory response once any error signal reaches a 3σ threshold in healthy young women asked to perform the maximal forward-reach task. Physical confirmation of the compensatory response is the execution of a compensatory step by the subject. A successfully predicted response is required to lag the instant of CEA by $\geq$100 ms but lead the compensatory response by no more than 2 s to ensure its specificity. The 100 ms value is based on the fastest measured volitional human response times (Mero and Komi 1990), whereas the 2 s value was kept the same as that used by Ahmed and Ashton-Miller (2004) for purposes of comparison. We also investigate the relative importance and sensitivity of each error signal, and the optimal threshold level, for detecting CEA. Finally, we compare the efficacy of the CEA approach for detecting a loss of balance with that of traditional methods involving kinematic thresholds or the position of the center of gravity relative to the base of support.

METHODS

CEA theory development and implementation

SAGITTALLY SYMMETRIC MODEL AND EQUATIONS OF MOTION OF THE FORWARD-REACH TASK. *Theory development.* To apply CEA theory to this task, and predict any compensatory step, the control error signals must be determined (i.e., errors in joint or segment position, velocity, or acceleration). Figure 1 demonstrates that the CEA detector needs two types of signals to calculate the error: the actual outputs and the internal model-predicted outputs. The actual outputs of the system are determined by the plant dynamics, which are defined by the corresponding equations of motion. Similarly, the predicted outputs are determined by the internal model, which is also based on the plant dynamics' equations of motion. Thus the model of the plant dynamics in this task will determine both the actual and predicted outputs, and hence, the control error signals.

Theory implementation. The reaching activity was modeled in the sagittal plane, as a three-link inverted pendulum (Kozak 1999; Kozak et al. 2003). The three rigid links represent the head, arms, and torso (HAT), both legs (LEG), and both feet (FOOT). The head, arms, and torso were treated as one segment due to the minimal relative motion observed between these segments in another forward reaching task (Kozak 1999; Kozak et al. 2003). This three-link kinematic chain was considered to pivot about the hip, ankle and metatarsal (toe) joints. The control inputs of interest obtainable from this analysis were the torques acting on the HAT, LEG, and FOOT segments. The outputs of interest were the angular accelerations of the individual body segments: HAT, LEG, and FOOT (Fig. 2).

The torques acting on each segment were computed using the equations of motion for this system and an inverse dynamics analysis. Kane's method produced the following equations of motion in the generalized coordinates $\boldsymbol{\theta}(t) = \{\theta_{HAT}(t)\ \theta_{LEG}(t)\ \theta_{FOOT}(t)\}$, and their derivatives

$$\mathbf{M}(\boldsymbol{\theta})\ddot{\boldsymbol{\theta}} = -\mathbf{T} - \mathbf{V}(\boldsymbol{\theta},\dot{\boldsymbol{\theta}}) \tag{1}$$

and in expanded form,

$$\begin{bmatrix} m_{11} & m_{12} & m_{13} \\ m_{21} & m_{22} & m_{23} \\ m_{31} & m_{32} & m_{33} \end{bmatrix} \begin{bmatrix} \ddot{\theta}_{HAT} \\ \ddot{\theta}_{LEG} \\ \ddot{\theta}_{FOOT} \end{bmatrix} = -\begin{bmatrix} t_1 \\ t_2 \\ t_3 \end{bmatrix} - \begin{bmatrix} v_1 \\ v_2 \\ v_3 \end{bmatrix} \tag{2}$$

The inertia matrix and torque and potential vectors are denoted by **M**, **T**, and **V,** respectively. **T** is the vector of torques relating to the generalized coordinates. **V** is in terms of anthropometric measures, $\boldsymbol{\theta}$ and $\dot{\boldsymbol{\theta}}$. **M** is a function of anthropometric measures (segment masses, lengths, center of mass locations, and moments of inertia) and $\boldsymbol{\theta}$. The generalized coordinates and their derivatives were obtained from the experimentally observed segment angles, angular velocities and accelerations.

NOMINAL FORWARD INTERNAL MODEL. *Theory development.* CEA theory assumes that the CNS is uncertain of the exact limits of stability in this task. One way to determine those limits is to identify an internal model of normal (or desired) system responsiveness to an input, and detect any deviations from this nominal level. These deviations, the errors between the actual and model-predicted outputs, are the signals of primary interest in this study (Fig. 1). Thus our goal is to obtain the model and corresponding matrix terms that characterize the system's nominal responsiveness to a given input. We further propose that this model may be self-identified on-line from experimental data.

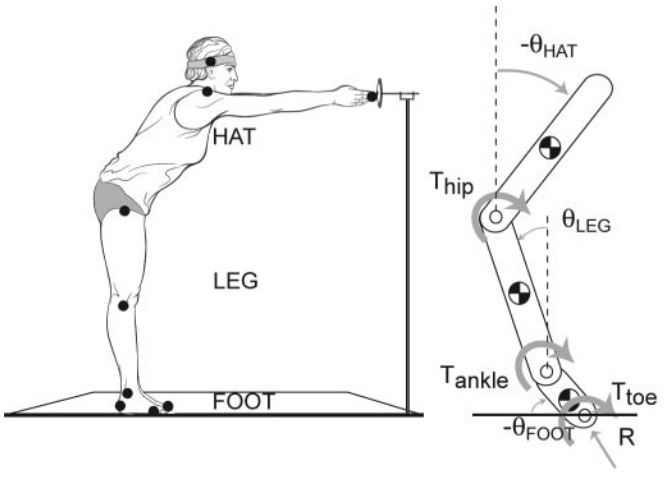

FIG. 2. Illustration of a subject performing a forward reach with raised heels (*left*), and the corresponding rigid-link model (*right*).

Theory implementation. The mathematical structure of the model needed to predict the expected outputs, body segment angular accelerations, was already defined by the equations of motion

$$\ddot{\boldsymbol{\theta}} = \mathbf{M}^{-1}(-\mathbf{T} - \mathbf{V}) \tag{3}$$

and in expanded form,

$$\begin{bmatrix} \ddot{\theta}_{HAT} \\ \ddot{\theta}_{LEG} \\ \ddot{\theta}_{FOOT} \end{bmatrix} = \begin{bmatrix} m_{11} & m_{12} & m_{13} \\ m_{21} & m_{22} & m_{23} \\ m_{31} & m_{32} & m_{33} \end{bmatrix}^{-1} \left(-\begin{bmatrix} t_1 \\ t_2 \\ t_3 \end{bmatrix} - \begin{bmatrix} v_1 \\ v_2 \\ v_3 \end{bmatrix} \right) \tag{4}$$

Because the inputs, **T,** and outputs, $\ddot{\boldsymbol{\theta}}$, were known, the approximations to matrices **M** and **V** may be identified in terms of constant coefficients using least-squares multiple linear regression. To identify the nominal internal model, however, a significant modification was made. To reliably predict the output signal, regression analysis was only applied to the frequency range of the input signal that provided the best characterization of the system response. The system's acceleration output was, compared with the torque inputs, primarily composed of higher-frequency harmonics. This can be explained by the dynamic response of the triple-inverted pendulum, where the lower-frequency torque inputs function to compensate for the destabilizing effect of gravity. Thus the resultant acceleration output was due to the higher-frequency torque inputs.

To quantify the internal model for the nominal response, the input torques were de-trended with a high-pass, no-lag filter at 0.6 Hz. Multiple linear regression was then employed to obtain the constant matrices $\tilde{\mathbf{M}}$, and $\tilde{\mathbf{V}}$, using the actual outputs and de-trended inputs, $\tilde{\mathbf{T}}$ as regressors over a time period of 2 s early in each trial (see *Eq. 5*). The de-trending frequency of 0.6 Hz approximates the −3 dB point of the linearized system's frequency response when the amplitude of the output response to the input has been reduced by 3 dB. Post hoc analysis confirmed that 95, 91, and 94% of the FOOT, LEG, and HAT acceleration power, respectively, were contained in frequencies >0.6 Hz.

Once the internal model parameters were identified, the predicted accelerations, $\hat{\ddot{\boldsymbol{\theta}}}(t) = \{\hat{\ddot{\theta}}_{HAT}(t)\ \hat{\ddot{\theta}}_{LEG}(t)\ \hat{\ddot{\theta}}_{FOOT}(t)\}$ were calculated using forward dynamics

$$\hat{\ddot{\boldsymbol{\theta}}} = \tilde{\mathbf{M}}^{-1}(-\tilde{\mathbf{T}} - \tilde{\mathbf{V}})$$

$$\begin{bmatrix} \hat{\ddot{\theta}}_{HAT} \\ \hat{\ddot{\theta}}_{LEG} \\ \hat{\ddot{\theta}}_{FOOT} \end{bmatrix} = \begin{bmatrix} \tilde{m}_{11} & \tilde{m}_{12} & \tilde{m}_{13} \\ \tilde{m}_{21} & \tilde{m}_{22} & \tilde{m}_{23} \\ \tilde{m}_{32} & \tilde{m}_{32} & \tilde{m}_{33} \end{bmatrix}^{-1} \left(-\begin{bmatrix} \tilde{t}_1 \\ \tilde{t}_2 \\ \tilde{t}_3 \end{bmatrix} - \begin{bmatrix} \tilde{v}_1 \\ \tilde{v}_2 \\ \tilde{v}_3 \end{bmatrix} \right) \tag{5}$$

The vector of error signals, $\mathbf{e}(t) = \{e_{HAT}(t)\ e_{LEG}(t)\ e_{FOOT}(t)\}$, was obtained for all points in time by calculating the difference between the actual and predicted accelerations

$$\mathbf{e} = \ddot{\boldsymbol{\theta}} - \hat{\ddot{\boldsymbol{\theta}}}$$

$$\begin{bmatrix} e_{HAT} \\ e_{LEG} \\ e_{FOOT} \end{bmatrix} = \begin{bmatrix} \ddot{\theta}_{HAT} \\ \ddot{\theta}_{LEG} \\ \ddot{\theta}_{FOOT} \end{bmatrix} - \begin{bmatrix} \hat{\ddot{\theta}}_{HAT} \\ \hat{\ddot{\theta}}_{LEG} \\ \hat{\ddot{\theta}}_{FOOT} \end{bmatrix} \tag{6}$$

One complication was that the internal model for the reach task could not be identified from the start of the trial. The task begins with a rapid forward movement of the body. Pilot studies showed that an internal model that accurately predicted motion throughout the trial could not be identified during this phase. We considered this initial movement to be feedforward in nature and that it was implemented by a different control strategy than the remainder of the trial. To avoid

poor internal model identification during this portion, a limit was therefore placed on the angular velocity and acceleration of the HAT segment. Self-identification commenced at the earliest time point in the trial when the HAT angular velocity in the forward direction was <0.1 rad/s and remained <0.2 rad/s for the following 1 s. Additionally, the angular acceleration of the HAT segment at this time point was required to be greater than zero.

CEA DETECTION. *Theory development.* A failure detection algorithm detects a CEA when one of the error signals, e, crosses a moving threshold set at 3 SD (3σ) above or below the mean of the baseline performance data.

Theory implementation. The error signal and the upper and lower thresholds from a representative reach trial are shown in Fig. 3. Also included in Fig. 3 are the following details. The internal model was identified using data in the 2 s window a. The performance data were obtained from b, a 4 s forward-moving trailing window, which lagged the current time instant, t, by 100 ms. The mean, μ_b, and SD, σ_b, obtained from this window were then used to calculate the threshold, e_{thresh}, at time t, 100 ms later (see *Eq. 8*). Calculation of the moving threshold commenced at "Start," initially using the 2 s of data prior as baseline data, with a 100 ms delay (δ) to allow for neural processing (van der Kooij et al. 1999). As time elapsed, the 2 s window expanded until a 4 s duration was obtained. This moving 4 s window, b, continued to move through the trial, calculating the threshold 100 ms later. A CEA was detected after the threshold had been crossed continuously for 100 ms, i.e.,

$$e(t) > \mu_b + 3\sigma_b \text{ continuously for past 100 ms} \quad (7a)$$

or

$$e(t) < \mu_b - 3\sigma_b \text{ continuously for past 100 ms} \quad (7b)$$

where

$$e_{thresh}(t) = \mu_b \pm 3\sigma_b \quad (8)$$

and μ_b was the mean, and σ_b was the SD of the trailing window

$$b = e(t - 4.1 \text{ s}) \cdot e(t - 0.1 \text{ s})$$

In other words, given a CEA at time t, e_{thresh} must have been exceeded from $(t - 0.2$ s) to $(t - 0.1$s).

Experiment design

Eleven healthy young women, aged 18–30 yr and with a mean height of 1.67 ± 0.07 (SD) m and mass of 60.72 ± 7.13 (SD) kg, volunteered for this experiment. The present study focused on women because gender differences in CEA detection were not observed in previous studies (Ahmed and Ashton-Miller 2004; 2005). All subjects gave written informed consent as approved by the institutional Internal Review Board.

Subjects stood bipedally, barefoot, in a sagittally symmetric, upright posture, with their arms extended horizontally (Fig. 2). Hands were placed together, with palms touching. Feet were oriented in the sagittal plane a comfortable distance apart. Subjects were asked to reach forward as far as they could with both hands. To precipitate a loss of balance in young adults, the task was designed to be more challenging than the functional reach test. To this end, subjects were allowed to lift their heels off the ground. However, they were asked not to bend their knees or separate their hands as they performed the task.

Two preliminary trials were recorded in which the subjects were asked to reach as far as they could pushing a circular target forward with their finger tips. They were asked to hold that maximal position for 5 s and then return to their original starting position. The maximum of these two reaches was defined as their maximum reach. For the subsequent trials, the circular target was randomly positioned at

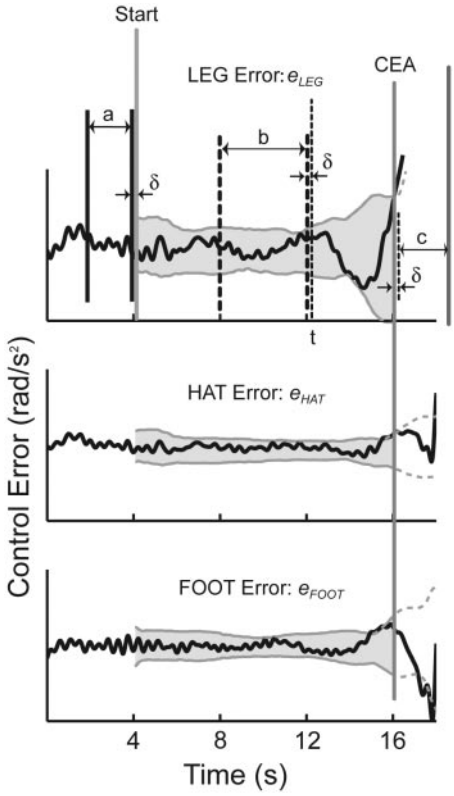

FIG. 3. Schematic of 3 control error signals: e_{LEG}, e_{HAT}, and e_{FOOT} (black) and 3σ thresholds (shaded). The 3σ algorithm is described on e_{LEG} (*top*). Internal model identification takes place in the 2 s window, a. This is followed, after 100 ms (δ), with the "Start" of the moving threshold calculation. The threshold at any time, t, is based on data in the moving, 4 s window, b. CEA is detected when the error signal crosses the 3σ threshold. For successful detection, a step must be initiated within the 2 s window, c, that follows CEA after a 100 ms delay (δ).

varying percentages of this maximum reach distance (95, 100, 105, 110, 115, 120, or 125%). In these trials, the subjects were instructed to attempt to reach the target and hold the position for as long as they could. After 10 s, they were asked to relax. The circular target was still free to slide, preventing the subjects from using it for support. If the subject managed to hold the position for 10 s, at a reach distance greater than her recorded maximum, this new reach distance was considered the new maximum reach and subsequent percentages were taken of it for placement of the target. Each subject performed trials until ten trials were recorded where a compensatory forward step had occurred. A spotter stood beside the subject to catch her in the event of a fall.

Data acquisition

Body segment orientation and location in three-dimensional space were measured at 100 Hz using infrared light-emitting diode (LED) markers and an Optotrak 3020 system (Northern Digital, Waterloo, Canada). Eight markers were placed on bony landmarks up the right side of the body, obtaining the kinematics of the foot, shank, thigh, torso and head (Fig. 2, *left*). One marker was placed on the left foot for step validation. Subjects stood with each foot on a separate six-channel forceplate (Model OR6-1000, AMTI, Watertown, MA). Three-dimensional ground reaction forces and moments were also recorded at 100 Hz.

The kinematic and force data were low-pass filtered with a cutoff frequency of 4 Hz using a fourth-order Butterworth filter (MATLAB, The MathWorks, Natick, MA). The angular position, velocity, and

acceleration of the HAT, LEG, and FOOT were calculated from the individual marker kinematic data. The filtered kinematics were differentiated using a five-point differentiation algorithm to obtain velocity and acceleration. All high- and low-pass filtering routines were employed forward and backward to minimize phase shift artifact.

Height, weight, and body segment lengths were measured for each subject. Segment inertial parameters were obtained using the tables provided in de Leva (1996).

Data analysis

STEP DETECTION. The occurrence of a step was defined as a compensatory response and evidence of CEA perception. Response time (RT) was calculated as the latency of this response following CEA. A step was defined to have been initiated when the absolute rate of change of the center of pressure in the frontal plane exceeded 10 cm/s and resulted in a step confirmed by visual examination.

SEGMENT KINEMATICS AND CONTROL ERRORS. Within-trial root-mean-squared (rms) and SD values of each segment's angular velocity and acceleration were calculated from the algorithm starting time to the time of step detection. The mean value of both measures were calculated for each subject and then compared across segments using a paired, two-sided, *t*-test ($P < 0.05$). Segment control error was compared using the same method.

CEA DETECTION FUNCTIONS. The 3σ algorithm, an algorithm that uses a moving, relative stochastic threshold set at 3 SD above the mean, was applied to all trials in which a compensatory step occurred. Because there were multiple error signals involved, we investigated the reliability of CEA using four alternative detection functions that specified which error signal, or combination thereof, was required to cross the threshold to trigger a detection. The FIRST function detected CEA when the first of the three segment acceleration control error signals reached the 3σ threshold. The remaining three functions, HAT, LEG, and FOOT, monitored only one acceleration control error signal (e_{HAT}, e_{LEG}, or e_{FOOT}, respectively) and detected a CEA when that specific error exceeded the 3σ threshold. Loss of balance was confirmed by the initiation of a step within 0.1–2 s of CEA detection. For comparison, the time from loss of balance to impact with the ground in a fall has been estimated at 0.7–1.0 s (Hsaio and Robinovitch 1998).

CANDIDATE KINEMATIC SIGNALS FOR USE IN THE DETECTION FUNCTIONS. We also wanted to examine whether the control error signal was unique in its ability to detect a loss of balance and predict a compensatory response. Potential signals that may also indicate a loss of balance and precipitate a change in control strategy are kinematic signals such as body position, velocity, and acceleration. We therefore applied the 3σ algorithm to the individual body segment angular velocity and acceleration signals, using the same four detection functions utilized in the CEA analysis: FIRST, HAT, LEG, and FOOT. For comparison, an absolute, fixed threshold was also applied to the body segment velocity and acceleration signals as has been used by Wu (2000). If the signal reached a predefined fixed value, a loss of balance was detected. The detection approaches, defined by the type of signal monitored and threshold implemented, are summarized in the first four columns of Table 1, along with the corresponding detection functions.

Finally, a third candidate kinematic signal, whole-body center of mass (COM) position, was monitored. This approach detected a loss of balance when the center of mass exceeded the limits of the base of support defined by both feet (see, for example, Pai et al. 2000). The base of support limits were calculated as a percentage of foot length. Three values for the limits were implemented, corresponding to 0, 10, and 35% of each subject's foot length measured posteriorly from the tip of the longest toe. The 35% value was obtained from the literature and reflects the fact that the anterior margin of the functional base of support does not extend to the tips of the toes and is correlated with toe flexor strength (Endo et al. 2002). To determine the optimal value, the intermediate limit of 10% was also investigated. Algorithm starting times were consistent for all detection approaches,

SENSITIVITY AND STATISTICAL ANALYSES. A sensitivity analysis was performed on all detection approaches and functions to determine the optimal relative (σ) and absolute (Abs) threshold level for successful response prediction. In the FIRST detection, where three signals are monitored, the threshold level was consistent for all signals. A χ^2 statistical test compared the success rates of the various detection functions, approaches and algorithm parameters with $P < 0.05$ considered statistically significant.

TABLE 1. *Loss of balance detection approaches: optimal threshold level, success rate at optimal threshold level, and mean response time (RT)*

Name	Signal	Threshold	Function	Optimal Level	Success, %	RT, ms
Control error anomaly	Control error	Relative (σ)	FIRST	3σ	89.8	967 (555)
			LEG	3σ	92.6	796 (532)
			HAT	2.7σ	74.1	947 (559)
			FOOT	2.4σ	77.8	803 (519)
σVelocity	Velocity	Relative (σ)	FIRST	2.7σ	74.1	665 (541)
			LEG	2.1σ	79.6	659 (534)
			HAT	1.5σ	50.0	856 (553)
			FOOT	1σ	46.3	953 (515)
σAcceleration	Acceleration	Relative (σ)	FIRST	1.9σ	58.3	713 (533)
			LEG	1.6σ	59.3	646 (528)
			HAT	0.5σ	48.1	1011 (552)
			FOOT	1.1σ	45.4	958 (566)
Absolute Velocity	Velocity	Absolute (Abs)	FIRST	0.1 rad/s	65.7	899 (517)
			LEG	0.05 rad/s	64.8	448 (403)
			HAT	0.05 rad/s	25.0	909 (500)
			FOOT	0.1 rad/s	30.6	893 (523)
Abs. Acceleration	Acceleration	Absolute (Abs)	FIRST	0.65 rad/s^2	29.6	989 (548)
			LEG	0.25 rad/s^2	26.9	618 (510)
			HAT	0.45 rad/s^2	14.8	763 (526)
			FOOT	0.65 rad/s^2	6.4	1007 (531)
Center of Mass	Center of Mass position	Absolute (Abs)	n.a	10% foot length	51.9	839 (510)

Response time values are means ± SD.

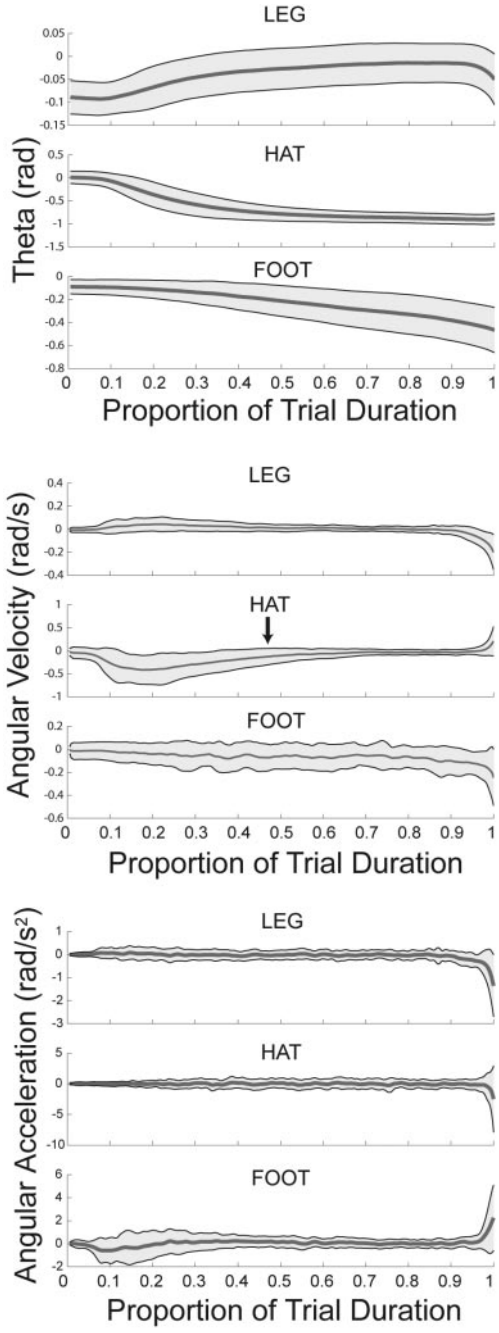

FIG. 4. Plots of LEG, HAT, and FOOT angles (*top*), angular velocities (*middle*), and angular accelerations (*bottom*) vs. normalized trial time, averaged across all stepping trials and all subjects. Trial time ends at the instant of step initiation. Shaded regions represent upper and lower 1 SD limits. A negative velocity reflects a forward angular velocity in the sagittal plane. The black arrow in the HAT angular velocity trace denotes the average time internal model identification commenced.

RESULTS

A total of 110 stepping trials were recorded (10/subject). Two trials were discarded for technical reasons. Averaged segment kinematics are presented in Fig. 4. The leg segment exhibited significantly less rms angular velocity and acceleration than the HAT or FOOT segments ($P < 0.001$). The mean ± SD rms angular velocities of the LEG, HAT, and FOOT segments were 0.036 ± 0.017, 0.069 ± 0.020, and 0.122 ± 0.044 rad/s, respectively. Variability in the LEG segment kinematics was also significantly less than that of the HAT or FOOT segments ($P < 0.001$). LEG rms control error was lower than that of the HAT or FOOT segments ($P < 0.001$). No differences were observed in control error variability between segments.

Loss of balance was successfully detected by CEA with a 3σ algorithm, using the FIRST function, in 89.8% of 108 trials, as evidenced by a compensatory response in the form of a forward step, with a response time (RT) between 100 ms and 2 s. On average, subjects stepped 7.54 ± 3.41 s after the trial began, and the mean duration between the start of CEA detection and the time of step initiation was 4.91 ± 3.16 s.

CEA proved to be more sensitive to certain error signals than other error signals. The application of the 3σ threshold to the LEG control error signal provided the highest success rate (92.6%) although not significantly greater than FIRST ($P = 0.427$). This difference was due to the false positive detections in the first function by the HAT and FOOT control errors. The LEG success rate of 92.6%, however, was greater than that provided by monitoring the HAT or FOOT control error signals ($P = 0.000$; Fig. 5).

Trials with a loss of balance successfully detected by CEA using the LEG function, had an average RT of 796.4 ± 532 (SD) ms. The response time distribution was skewed toward 100 ms with >50% of the trials exhibiting a response time of <700 ms (Fig. 6). In the remaining eight trials where CEA was not detected successfully, three of these failures were a result of a false positive detection error. The algorithm falsely detected a CEA much earlier, >2 s, before the actual step was initiated. Steps in five trials were detected too late. In comparison, the HAT and FOOT detection functions had 25 and 30 false negative detections, respectively. This result shows that a detection function that required all three error signals to cross the threshold for CEA detection would have had ≥30 false negative detections.

A threshold value of 3σ provided the optimal success rate using the LEG and FIRST detection functions. Threshold values above or below this led to decreased sensitivity and specificity, respectively, of CEA detection (Fig. 7). The optimal thresholds values for the HAT and FOOT functions were slightly lower.

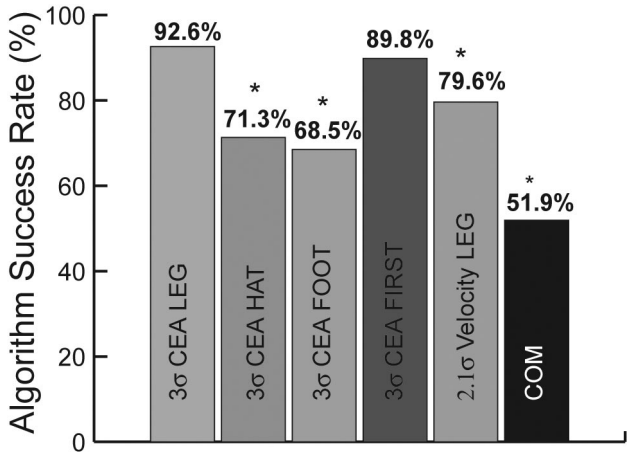

FIG. 5. Algorithm success rates for 3σ CEA, Velocity, and Center of mass (COM) detection approaches. (*: χ^2 probability, P, relative to 3σ CEA LEG <0.01).

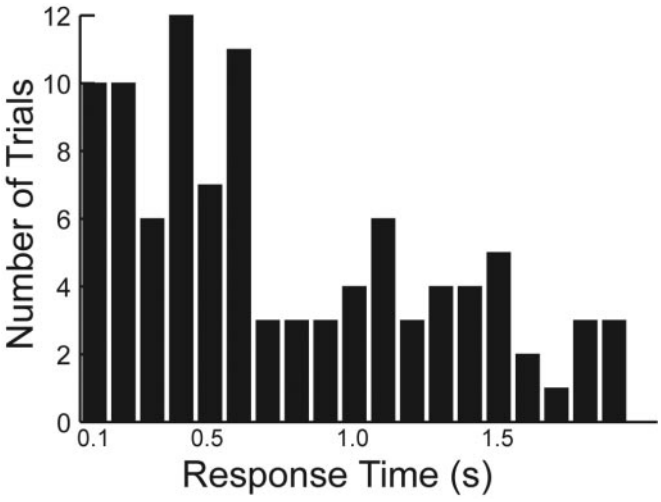

FIG. 6. Response time distribution for 3σ CEA LEG successfully predicted responses.

The results of both CEA and kinematic detection approaches are presented in Table 1. A sensitivity analysis was conducted on both the relative (σ) and absolute (Abs) threshold level and the values reported are those obtained at the optimal threshold levels for predicting a compensatory response. All candidate kinematic detection approach/function combinations predicted a compensatory step significantly less reliably than CEA using either LEG or FIRST detection functions ($P = 0.000$, $P < 0.03$, respectively). Nine approach/function combinations performed similarly to either the HAT or FOOT CEA detection functions ($P > 0.05$).

DISCUSSION

The present results show that a self-identified, internal, on-line model of the nominal interaction of the body with its environment can be used to detect a loss of balance. It is novel that the loss of balance was detectable without knowledge of the whole body center of gravity location relative to its base of support. Because all the input and output parameters monitored are typically available to the CNS, which is hypothesized to use internal models in other contexts (see INTRODUCTION), the results suggest that the CNS may use a scheme involving a nominal forward internal model and CEA to detect a loss of balance and trigger the compensatory response.

The optimal threshold value for CEA detection was 3σ in this multi-degree-of-freedom, forward reach task. This was true when using the LEG and FIRST CEA detection functions, the two functions that were most reliable in predicting a compensatory response. This implies that it is the anomalous value of the error signal that triggers the compensatory response. From the subject's point of view, a lower threshold would have increased the available response time but resulted in unnecessary responses. Conversely, a higher threshold would make it more difficult to recover balance by reducing the available time for a response that was guaranteed to be mandatory. Thus the existence of an optimal threshold also may represent the tradeoff that exists between increased caution and increased risk-taking on the part of the subject.

Effect of control error detection functions on CEA

Successful detection of loss of balance by CEA was not dependent on all of the control error signals crossing the threshold. In fact, by monitoring only one of the control errors, better detection reliability could be obtained. It was surprising that error in the control of the HAT acceleration appeared relatively unimportant, despite it containing ~60% of the body's mass as well as the vestibular system with its position, rate, and acceleration detectors. On the other hand, error in the control of LEG angular acceleration had great importance in the successful detection of CEA. There are at least three possible explanations for this result. First the CNS may indeed preferentially control LEG segment angular acceleration. This is supported by the minimal within-trial rms value and variability of the angular velocity and acceleration of the LEG segment, whereas the HAT and FOOT segments exhibited significantly greater values (Fig. 4). Furthermore, LEG control error was less than HAT and exhibited a trend toward lower error than the FOOT. These results may indicate an effort by the CNS to control the LEG segment. Functionally, this may be explained by the stabilizing role the LEG segment plays to counteract the dynamics induced by the goal-directed forward movement of both the HAT and FOOT. A second explanation is that the lower velocity of the LEG segment may also allow the identification of an internal model with less modeling error, resulting in lower control error signals and greater success rates. The greater reliability of the LEG segment in detecting a loss of balance may be the result of a more accurate model. A third possibility is that LEG control error appears important simply because it is the first indicator of a loss of balance. Indeed, the FIRST detection function performed as well as the LEG detection function. This is because the LEG was usually the first function to detect a CEA, ahead of the HAT or FOOT functions. This is further supported by results of the LEG velocity detection function in that LEG velocity was a better predictor of loss of balance than HAT or FOOT velocity. Future work might further investigate the significance of the LEG segment, in addition to combinations of error signals, in the initiation of a compensatory response.

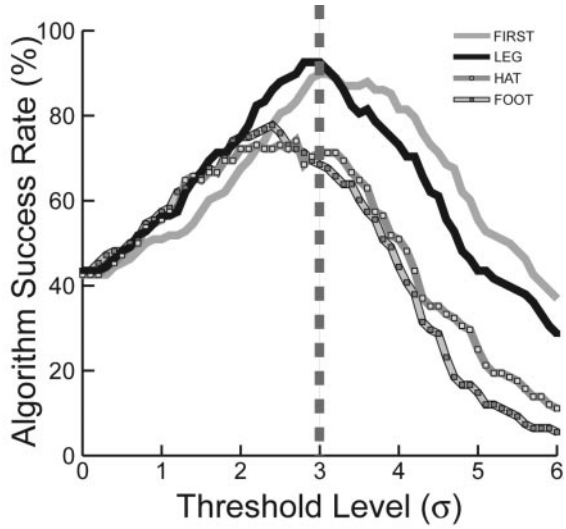

FIG. 7. Sensitivity of CEA algorithm to relative threshold level (σ). - - -, 3σ, the optimal threshold for FIRST and LEG detection functions.

Comparison of CEA with kinematic loss of balance detection approaches

The CEA algorithm was a better loss of balance detector and step predictor than any of the traditional kinematic signals that have been used to detect a loss of balance hitherto, including center of gravity location relative to the base of support (Pai and Patton 1997; Wu 2000). Monitoring velocity of the LEG segment with a relative threshold of 2.1σ also performed reasonably well, although significantly less reliably than a 3σ threshold on LEG control error. In addition, although 3σ has been successfully applied to both a reach and chair balance tasks, the 2.1σ threshold on segment velocity does not generalize to both tasks due to their different characteristic velocity profiles. Moreover, the relatively high step prediction success obtained by monitoring LEG velocity may be a consequence of the quasi-static nature of the reach task, especially that of the LEG segment.

Is segment acceleration sensation available to the CNS?

In the 1 df chair-balancing task studied by Ahmed and Ashton-Miller (2004), the acceleration signal monitored was directly available to the CNS by way of vestibular afference. On the other hand, although segmental velocity and position are available from muscle spindle afference in the reach task, there appears to be no physiological sensor specific to segment angular acceleration. It is possible, however, that angular acceleration could be derived from muscle forces sensed by the Golgi tendon organs or by differentiation of the velocity information provided by the muscle spindles. Thus it is conceivable that the CNS has access to segmental acceleration. A number of computational studies on internal models and postural control have made similar assumptions and provide evidence of acceleration predictions by forward internal models (for example, Flanagan and Lolley 2001; McIntyre et al. 2001). It is also important to note that the CEA theory is not restricted to acceleration control error in that it can be implemented using velocity or position control error. Acceleration control error was used in this task because it facilitated the identification of an accurate internal model using a structure based on the equations of motion. We believe that the CEA theory may have been more successful than traditional approaches in predicting stepping because it incorporated control inputs in decision making.

Significance of a nominal internal model

Clearly the use of an exact internal model of the system in this analysis would have been inadequate because it would simply calculate the natural progression of fall kinematics with no resultant error signal. CEA theory is based on the predicted outputs of a model of the system in a nominal operating state, thus any deviation from this state will be detected. As a result, the internal model identified is local to this operating region. This idea has been supported by a number of studies showing that learned internal models only show limited generalization across the workspace (Gandolfo et al. 1996; Shadmehr 2004).

The method for identifying the nominal model, including the focus on high-frequency input/output dynamics is a subject of ongoing research. The performance of models that focus on the low-frequency dynamics, models with parameters that are continuously updated and models that incorporate trailing observers that are dependent on past states are also under investigation.

Limitations

Limitations include the fact that an internal model could not be accurately identified for rapid or ballistic movements as well as for movements over large ranges of motion. The ability to predict the segment accelerations at the start of each trial, where there is a ballistic movement, was therefore poor; the system needed to reach and maintain a steady state. If the subject did not slow down, the control error would be artificially large. Further limiting the analysis was our identification and use of a single internal model as opposed to multiple models. It has been suggested that the CNS maintains multiple internal models and uses them to identify the current context and plan its movements appropriately (Wolpert and Kawato 1998). Accordingly, a more general application of the CEA theory would not solely detect a loss of balance in the context of a fall. In the presence of multiple internal models, CEA would detect a loss of control of the current internal model and would trigger a change in control strategy to regain control of the system.

A limitation of the experimental protocol was that if subjects successfully reached the target and held it for ~10 s without a loss of balance, they returned to their initial position even if the data collection period had not yet elapsed. These successful trials should have been ideal for analyzing the reliability of CEA in not predicting a step when there was no step as well as step prediction if there was a step. Unfortunately, for these no-step trials, we cannot be sure of the exact instant when subjects changed their control strategy and started to return to their initial configuration. Thus a CEA could have been detected in the absence of a step due to the subject's initiation of a new motor program. A future study should ensure that successful trials that do not exhibit a loss of balance are carried out for the duration of the data collection period, eliminating the possibility of a novel motor program being initiated.

Finally, our ability to validate the criterion used to detect a loss of balance is limited by the variability in the subsequent response time, which can result from a number of factors. The longer response times observed may have been a result of subject habituation. Although a step was required to recover from a loss of balance, once the subjects became familiar with the task, they realized that the response need not be immediate. They may also be a result of lower velocities and accelerations. For example, Nashner et al. found an inverse relationship between response times and postural sway rate and observed response times on the order of 1.4 s (Nashner 1971). Another possibility is that the increased response times may reflect a choice reaction time, which increases with the number of choices available (Kandel et al. 2000). The use of the 2-s criterion on successful step prediction, which was based on a previously analyzed task, may also have affected the accuracy with which some compensatory responses could be predicted.

Conclusions

The present results support the hypothesis that a loss of balance is a loss of effective control of balance as evidenced by

a probabilistically unusual error between predicted and actual sensory consequences of a movement. A scheme involving a self-identified, nominal internal model, monitoring of control input and error, and stochastic decision making can be used to detect a loss of balance and predict a compensatory response in a complex, multiple-input, multiple-output task.

ACKNOWLEDGMENTS

We are grateful for the assistance of S. Brock, A. Figueroa, J. Kemp, and M. Stenzel. We also thank two anonymous reviewers and D. Wolpert for helpful comments.

GRANTS

This research was supported by National Institute on Aging Grants P01 AG-10542 and P30 AG-08808, a Multidisciplinary Research Training in Aging Grant T32 AG-00116 to A. Ahmed and a Biology of Aging Training Grant T32 AG-000114-21 to A. Ahmed.

REFERENCES

Ahmed AA, Ashton-Miller JA. Is a "loss of balance" a control error signal anomaly? Evidence for three-sigma failure detection in young adults. *Gait Posture* 19: 252–262, 2004.

Ahmed AA, Ashton-Miller JA. Effect of age in detecting a loss of balance in a seated whole body balancing task. *Clin Biomech* 20: 767–775, 2005.

Blakemore SJ, Frith CD, Wolpert DM. The cerebellum is involved in predicting the sensory consequences of action. *Neuroreport* 12: 1879–1884, 2001.

Blakemore SJ, Oakley DA, Frith CD. Delusions of alien control in the normal brain. *Neuropsychologia* 41: 1058–1067, 2003.

Blakemore SJ, Wolpert DM, Frith CD. Central cancellation of self-produced tickle sensation. *Nat Neurosci* 1: 635–640, 1998.

Botvinick MM, Cohen JD, Carter CS. Conflict monitoring and anterior cingulate cortex: an update. *Trends Cogn Sci* 8: 539–546, 2004.

Cham R, Redfern MS. Changes in gait when anticipating slippery floors. *Gait Posture* 15:2: 159–171, 2002.

de Leva P. Adjustments to Zatsiorsky-Seluyanov's segment inertia parameters. *J Biomech* 29: 1223–1230, 1996.

Diedrichsen J, Verstynen T, Lehman SL, Ivry RB. Cerebellar involvement in anticipating the consequences of self-produced actions during bimanual movements. *J Neurophysiol* 93: 801–812, 2005.

Duncan PW, Weiner DK, Chandler J, Studenski S. Functional reach: a new clinical measure of balance. *J Gerontol* 45: M192–197, 1990.

Endo M, Ashton-Miller JA, Alexander NB, Effects of age and gender on toe flexor muscle strength, *J Gerontol* 57A: M392–M397, 2002.

Eng JJ, Winter DA, Patla AE. Strategies for recovery from a trip in early and late swing during human walking. *Exp Brain Res 102:* 2: 339–349, 1994.

Flanagan JR, Lolley S. The inertial anisotropy of the arm is accurately predicted during movement planning. *J Neurosci* 21: 1361–1369, 2001.

Gandolfo F, MussaIvaldi FA, Bizzi E. Motor learning by field approximation. *Proc Natl Acad Sci USA* 93: 9: 3843–3846, 1996.

Hohwy J, Frith C. Can neuroscience explain consciousness? *J. Consc Studies* 11: 7-8: 180–198, 2004.

Hsiao ET, Robinovitch SN. Common protective movements govern unexpected falls from standing height. *J Biomech* 31: 1–9, 1998.

Kandel ER, Schwartz JH, Jessel TM, Schwartz JH, Jessel TM. *Principles of Neural Science.* New York: McGraw-Hill, 2000.

Kerns JG, Cohen JD, MacDonald AW, Cho RY, Stenger VA, Carter CS. Anterior cingulate conflict monitoring and adjustments in control. *Science* 303: 1023–1026, 2004.

Kording KP, Wolpert DM. Bayesian integration in sensorimotor learning. *Nature* 427: 244–247, 2004.

Kozak K. *On the Control of Balance During the Performance of a Forward Reach: Effects of Age, Biomechanical and Psychological Factors* (PhD dissertation). Ann Arbor, MI: University of Michigan, 1999.

Kozak K, Ashton-Miller JA, Alexander NB. The effect of age and movement speed on maximum forward reach from an elevated surface: a study in healthy women. *Clin Biomech* 18: 190–196, 2003.

Loram ID, Maganaris CN, Lakie M. Paradoxical muscle movement in human standing. *J Physiol* 556: 683–689, 2004.

Lungu OV, Wachter T, Liu T, Willingham DT, Ashe J. Probability detection mechanisms and motor learning. *Exp Brain Res* 159: 135–150, 2004.

Maki BE, Norrie RG, Zecevic A, Quant S, Kirshenbaum N, Bateni H, McIlroy WE. Initiation and execution of rapid postural reactions and stepping movements: which phases require visuospatial attention? In: *Control of Posture and Gait*, edited by Duysens J, Smits-Engelsman BCM and Kingma H. Maastricht: International Society for Posture and Gait Research, 2001a, p. 573–576.

Maki BE, Zecevic A, Bateni H, Kirshenbaum N, McIlroy WE. Cognitive demands of executing postural reactions: does aging impede attention switching? *Neuroreport* 12: 3583–3587, 2001b.

Marr D. A theory of cerebellar cortex. *J Physiol* 202: 437–470, 1969.

McIlroy WE, Norrie RG, Brooke JD, Bishop DC, Nelson AJ, Maki BE. Temporal properties of attention sharing consequent to disturbed balance. *Neuroreport* 10: 2895–2899, 1999.

McIntyre J, Zago M, Berthoz A, Lacquaniti F. Does the brain model Newton's laws? *Nat Neurosci* 4: 693–694, 2001.

Mero A, Komi PV. Reaction time and electromyographic activity during a sprint start. *Eur J Appl Physiol Occup Physiol* 61: 73–80, 1990.

Muller F, Dichgans J. Dyscoordination of pinch and lift forces during grasp in patients with cerebellar lesions. *Exp Brain Res* 101: 485–492, 1994.

Nashner LM. A model describing vestibular detection of body sway motion. *Acta Otolaryngol* 72: 429–436, 1971.

National Center for Injury Prevention and Control. *Activity Report 2001 CDC's Unintentional Injury Prevention Program.* Atlanta: Centers for Disease Control and Prevention, National Center for Injury Prevention and Control, 2002.

Ouchi Y, Okada H, Yoshikawa E, Nobezawa S, Futatsubashi M. Brain activation during maintenance of standing postures in humans. *Brain* 122: 329–338, 1999.

Pai YC, Maki BE, Iqbal K, McIlroy WE, Perry SD. Thresholds for step initiation induced by support-surface translation: a dynamic center-of-mass model provides much better prediction than a static model. *J Biomech* 33: 387–392, 2000.

Pai YC, Patton J. Center of mass velocity-position predictions for balance control. *J Biomech* 30: 4: 347–354, 1997 [published erratum appears in *J Biomech* 31: 199, 1998].

Powell LE, Myers AM. The Activities-specific Balance Confidence (ABC) Scale. *J Gerontol A Biol Sci Med Sci* 50A: M28–34, 1995.

Rice D, MacKenzie E. *Cost of Injury in the United States: A Report to Congress.* Baltimore, MD: Injury Prevention Center, The John Hopkins University, Institute for Health and Aging, University of California, San Francisco, CA, 1989.

Shadmehr R. Generalization as a behavioral window to the neural mechanisms of learning internal models. *Hum Mov Sci* 23:5: 543–568, 2004.

Tinetti ME, Richman D, Powell L. Falls efficacy as a measure of fear of falling. *J Gerontol* 45: P239–243, 1990.

van der Kooij H, Jacobs R, Koopman B, Grootenboer H. A multisensory integration model of human stance control. *Biol Cybern* 80: 299–308, 1999.

van der Kooij H, Jacobs R, Koopman B, van der Helm F. An adaptive model of sensory integration in a dynamic environment applied to human stance control. *Biol Cybern* 84: 103–115, 2001.

Wolpert DM, Kawato M. Multiple paired forward and inverse models for motor control. *Neural Network* 11: 1317–1329, 1998.

Wu G. Distinguishing fall activities from normal activities by velocity characteristics. *J Biomech* 33: 1497–1500, 2000.